Rotationally resolved spectra of transitions involving methyl torsion and C–C–O bend of acetaldehyde in the system of $\tilde{A}^1A''-\tilde{X}^1A'$

Yung-Ching Chou, Cheng-Liang Huang, and I-Chia Chen[a)]
Department of Chemistry, National Tsing Hua University, Hsinchu, Taiwan 30013, Republic of China

Chi-Kung Ni and A. H. Kung
Institute of Atomic and Molecular Sciences, Academia Sinica, P.O. Box 23-166, Taipei, Taiwan 106, Republic of China

(Received 17 August 2001; accepted 11 October 2001)

In the fluorescence excitation spectrum of acetaldehyde cooled in a supersonic jet, we performed a full rotational analysis of combination bands $10_0^1 14_0^{0+} 15_0^n$ and $10_0^1 14_0^{0-} 15_0^n$, $n=0-4$ in the system $\tilde{A}^1A''-\tilde{X}^1A'$. The vibrational frequency of the C–C–O bending mode is determined to be $\nu'_{10}=373.163(3)$ cm^{-1}. The rotational structures of combination bands $10_0^1 14_0^{0+} 15_0^2$, $10_0^1 14_0^{0-} 15_0^2$, $10_0^1 14_0^{0+} 15_0^3$, and $10_0^1 14_0^{0-} 15_0^4$ resemble the structures of $14_0^{0+} 15_0^2$, $14_0^{0-} 15_0^2$, $14_0^{0+} 15_0^3$, and $14_0^{0-} 15_0^4$, respectively, but the intense *E* lines observed for $14_0^{0-} 15_0^3$ are not found in $10_0^1 14_0^{0-} 15_0^3$. Torsional spacings observed in the C–C–O bend series are slightly smaller than those in the pure torsional series 14^{0+} and 14^{0-}; these result from a decreased torsional barrier due to the C–C–O bending motion. Inversion spacings exhibit a pattern similar to those in the series 14^{0+} and 14^{0-}. Reversed abnormal torsional sublevel A/E splittings are found for states $n=0-2$ of the $10^1 14^{0-}$ series, similar to those in the 14^{0-} series. For states $n=3$, the *K* rotational structures between the 14^{0+} and $10^1 14^{0+}$ series and for $n=4$, the 14^{0-} and $10^1 14^{0-}$ series are more similar than those between the pure torsion-inversion series 14^{0+} and 14^{0-}. Hence, these experimental data imply that the interaction of the C–C–O bend with rotational structures of torsional states is smaller than that resulting from the aldehyde inversion. © *2002 American Institute of Physics.*
[DOI: 10.1063/1.1424312]

I. INTRODUCTION

In this laboratory we recorded the laser-induced fluorescence (LIF) spectrum of acetaldehyde in a supersonic jet for the system $\tilde{A}^1A''-\tilde{X}^1A'$ at resolution 0.02 cm^{-1} for the range from near the origin of $\tilde{A}^1A''$ to the vibrational energy ~1800 cm^{-1}; experimental details have been described previously.[1] In the upper state of this system $\tilde{A}^1A''$, acetaldehyde has significant alteration of its molecular geometry such that the methyl group converts from an eclipsed to a staggered conformation with respect to the O atom, and the aldehyde moiety distorts into a pyramidal conformation. State $\tilde{A}^1A''$ has essentially C_1 symmetry instead of C_s, as found in the electronic ground state. The Franck–Condon-active vibrations at small excitation energy involve torsion and inversion. In the preceding paper,[1] we reported a full rotational analysis of vibronic band series $14_0^{0+} 15_0^n$ and $14_0^{0-} 15_0^n$, $n=0-4$; vibrational mode Q_{14} denotes wagging of the aldehyde hydrogen and Q_{15} the methyl torsion; 14^{0+} and 14^{0-} denote the two inversion tunneling components of the aldehyde hydrogen bending out of plane in the vibrational ground state of $\tilde{A}^1A''$.[1–3] The height of the torsional barrier is estimated to be 650–660 cm^{-1}. Torsion-rotational interaction is found to affect the rotational structure of electronic bands that involve torsional vibronic levels below, near, and above the torsional barrier.

Acetaldehyde is a prototypical molecule for study of internal rotation of the methyl moiety. Many researchers have studied the torsional problem in its electronic ground state.[4–14] In the first electronically excited state, interaction of the inversion motion Q_{14} of the aldehyde hydrogen varies the torsional spacing and rotational *K* structures; for the 14^{0-} series, torsional levels with vibrational quantum numbers $v_t=0-2$ display reversed abnormal A/E sublevel splittings.[1,15–17] Our previous work shows that even torsional levels within the 14^{0+} series cannot be fitted with a program involving only a rotational and torsional Hamiltonian to obtain accurate parameters to represent potential energy.[1] The model of internal-rotation Hamiltonian and related theories about torsion-rotational motion, particularly for acetaldehyde, are described in detail elsewhere.[4–14]

Interaction between a large-amplitude torsional motion and other vibrations is observed in other molecules such as methanol,[18] 1-methylnapthalene,[19,20] acetone,[21] etc. Tan *et al.*[19,20] reported the effect of other vibrational modes on torsional motion in 1-methylnapthalene; the A/E splitting and degeneracy splitting differ from those in the vibrational ground state. Wang and Perry[18] reported similar behavior for the asymmetric C–H stretching modes in methanol. Liu *et al.*[15] performed quantum-chemical calculations on acetaldehyde potentials involving three motions—torsion, inver-

a)Author to whom all correspondence should be addressed. Electronic mail: icchen@mx.nthu.edu.tw

sion, and C–C–O deformation; their results imply significant interaction among these motions. These results cause some theoretical difficulties for a full understanding of the spectroscopic problem.

The vibrational progression next in energy for the electronically excited state of acetaldehyde is the combination bands involving C–C–O bend, the Q_{10} vibrational mode. Nobel and Lee[22] assigned some combination progressions of upper states based on LIF spectra of the jet-cooled isotopomers CH_3CHO, CH_3CDO, CD_3CHO, and CD_3CDO. Baba *et al.*[2] assigned many vibronic bands, with some involving C–C–O bending for two isotopic acetaldehydes CH_3CHO and CD_3CDO, but their C–C–O vibrational assignments differ significantly from previous assignments.[22] Liu *et al.*[15,16] recorded spectra at high resolution and performed rotational analysis on 20 vibrational bands, among which they assigned four C–C–O bending states; their assignments agree better with those made by Nobel and Lee.[22] In this laboratory, investigation of torsion-inversion levels taking into account torsion-rotational interaction,[1] enabled reassignment of many $E-E$ transitions made by Liu *et al.*;[15,16] furthermore, transitions originally assigned by Liu *et al.*[15] to $10_0^1 14_0^{0+}$ were reassigned to be part of $14_0^{0-}15_0^2$. For this reason it is important to analyze the torsion-rotational structures to determine the vibrational states; performing this analysis allows us to understand the variation of rotational structures and torsional spacing resulting from interaction of the two large amplitude motions and a vibrational motion with low frequency.

In the present work we analyzed the full rotational structure of vibrational progressions involving the C–C–O bend to energy about 1000 cm^{-1} above the origin of $\tilde{A}^1A''$. Combination bands $10_0^1 14_0^{0+} 15_0^n$ and $10_0^1 14_0^{0-} 15_0^n$ for $n=0-4$ are assigned. The effect of bending motion on rotational structures and torsional levels for two inversion-tunneling components 14^{0+} and 14^{0-} is discussed.

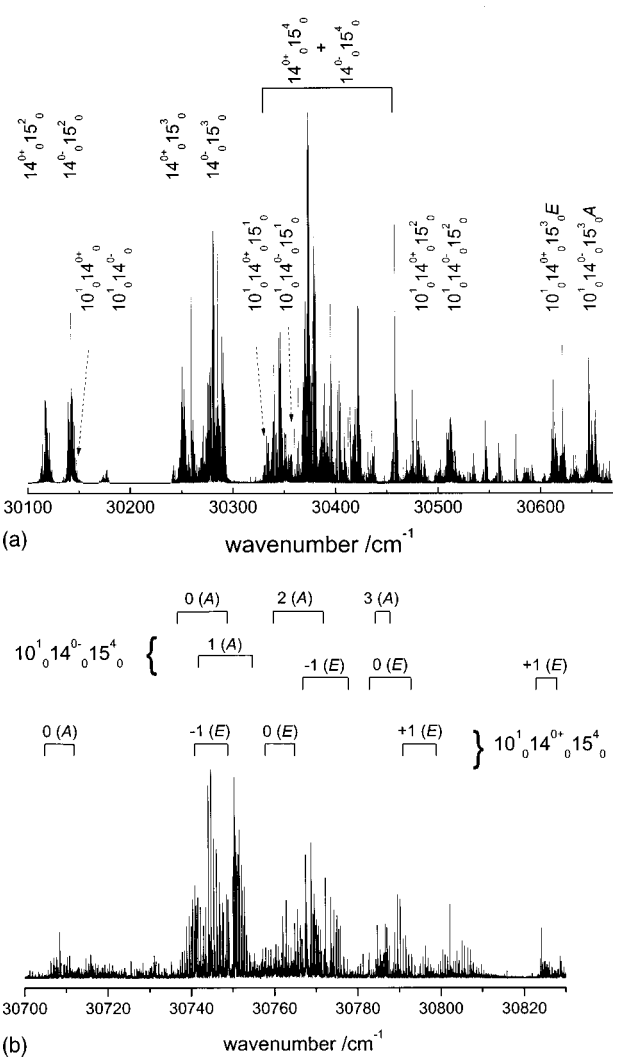

FIG. 1. Spectra and vibrational assignments for $\tilde{A}^1A''-\tilde{X}^1A'$ of CH_3CHO for excitation in regions (a) 30 100–30 660 cm^{-1} and (b) 30 700–30 830 cm^{-1} showing the progressions $10_0^1 14_0^{0+} 15_0^n$ and $10_0^1 14_0^{0-} 15_0^n$ with $n=0-4$. In (b) the K' quantum number is shown.

II. RESULTS AND DISCUSSION

We have observed new vibrational progressions starting from excitation frequency 30 100 to 30 830 cm^{-1}, as shown in Fig. 1; they display spacing, rotational structure, and band type similar to those in progressions $14^{0+}15^n$ and $14^{0-}15^n$. These characteristics indicate that the new vibrational mode involved has symmetry A'. In agreement with results of other research groups, we assigned these combination progressions as the series $10^1 14^{0+} 15^n$ and $10^1 14^{0-} 15^n$ involving angular deformation of the C–C–O group. Some features of the new vibrational progression resemble those of $14_0^{0+}15_0^n$ and $14_0^{0-}15_0^n$; for instance, rotational structures of $10_0^1 14_0^{0+} 15_0^2$, $10_0^1 14_0^{0-} 15_0^2$, $10_0^1 14_0^{0+} 15_0^3$, and $10_0^1 14_0^{0-} 15_0^4$ resemble those of $14_0^{0+}15_0^2$, $14_0^{0-}15_0^2$, $14_0^{0+}15_0^3$, and $14_0^{0-}15_0^4$, respectively, as shown in Figs. 2 and 3. This resemblance allows us to distinguish the 10^1 series from other series in the high-energy region. The abnormal transitions ($\Delta K_a=0$, $\Delta K_c=0$) appearing in A sublevels for $14_0^{0-}15_0^3$ and $14_0^{0+}15_0^4$ are also observed in band $10_0^1 14_0^{0-} 15_0^3$, as shown in Fig. 4. Because in $10_0^1 14_0^{0+} 15_0^4$ the A lines are weak, only a

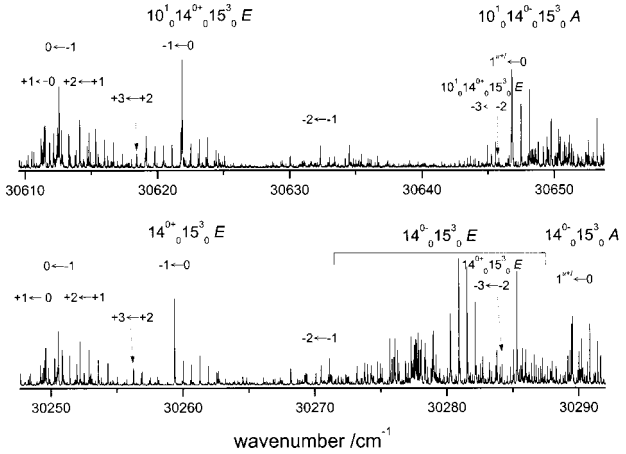

FIG. 2. Portion of spectra in ranges 30 610–30 655 cm^{-1} (upper) and 30 250–30 290 cm^{-1} (lower) for $10_0^1 14_0^{0-} 15_0^3$ and $14_0^{0-}15_0^3$, respectively. The E lines of $10_0^1 14_0^{0-} 15_0^3$ disappear but they are intense in $14_0^{0-}15_0^3$. Transitions $K'-K''$ are shown in the plot.

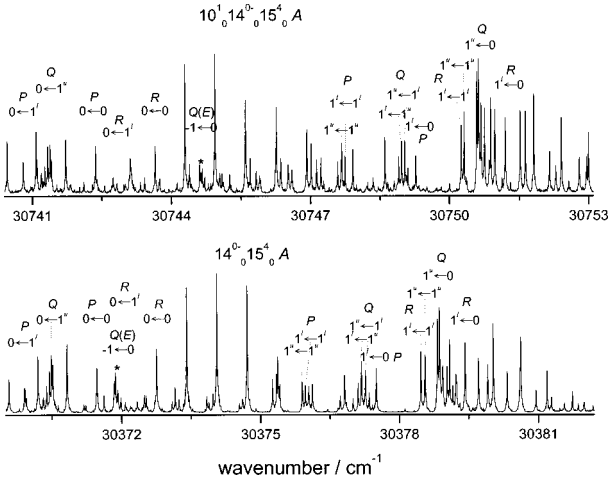

FIG. 3. Portion of spectra in ranges 30 740–30 753 cm^{-1} (upper) and 30 368–30 382 cm^{-1} (lower) for $10_0^1 14_0^{0-} 15_0^4$ and $14_0^{0-} 15_0^4$, respectively, showing similar rotational structures. Transitions $K'-K''$and $\Delta J=-1,0,+1$ for *P*, *Q*, and *R* branches are indicated. Symbol * denotes $14_0^{0+} 15_0^4(E)$ and $10_0^1 14_0^{0+} 15_0^4(E)$ for the lower and upper spectrum, respectively.

few lines are assigned; abnormal transitions, which are expected to be weaker than these *A* lines, are not assigned under current experimental conditions.

Some deviations are observed for the 10^1 series; the intense $E-E$ lines in $14_0^{0-} 15_0^3$ disappear in band $10_0^1 14_0^{0-} 15_0^3$, as displayed in Fig. 2. The *K* structures for $10_0^1 14_0^{0-} 15_0^4$ and $14_0^{0-} 15_0^4$ are similar, but not those for $10_0^1 14_0^{0+} 15_0^4$ and $14_0^{0+} 15_0^4$. In fact, comparison of their rotational structures indicates a closer similarity of $10_0^1 14_0^{0+} 15_0^4$ to $14_0^{0-} 15_0^4$ than to $14_0^{0+} 15_0^4$.

As described previously, because an adequate Hamiltonian is lacking, most assignments are based on known combination differences of rotational levels in the electronic ground state. To confirm assignments for *A* sublevels, we used a Hamiltonian based on an asymmetric rotor with a rotational parameter *A* affected by torsional motion; rotational parameters *B* and *C* are not affected by torsion and should reflect the geometric information. Detailed description for individual bands is given below. Because of widely spread *K* structures for bands $10_0^1 14_0^{0+} 15_0^4$ and $10_0^1 14_0^{0-} 15_0^4$, assignments for those *K* states are made differently from the others and are discussed together. The band origins, listed in Table I, are calculated from fits to an asymmetric rotor for the *A* sublevels or with a Hamiltonian involving internal rotor for the *E* sublevels. Some origins are determined directly from transitions to $J'_{KaKc}=0_{00}$. Table II lists the effective rotational parameters obtained for *A* sublevels from our best-fits to the asymmetric rotor Hamiltonian.

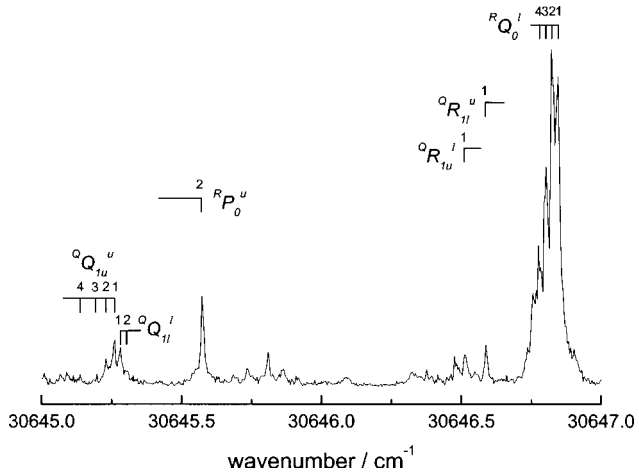

FIG. 4. Part of spectrum and assignments of band $10_0^1 14_0^{0-} 15_0^3$ showing forbidden $A-A$ transitions ${}^Q Q_{1u}^u(J_{1J-1}-J_{1J-1})$, ${}^Q Q_{1l}^l(J_{1J}-J_{1J})$, ${}^Q R_{1l}^u((J+1)_{1J}-J_{1J})$, and ${}^Q R_{1u}^l((J+1)_{1J+1}-J_{1J-1})$.

To label $A-A$ transitions we use the K_a, K_c convention for asymmetric rotors; in addition, upper and lower states of *K* doublets are denoted K^u and K^l, respectively. For an *E* sublevel, $+K$ denotes a degenerate pair $(\sigma,K)=(+1,+K)$ and $(-1,-\mathrm{K})$ and $-K$ pair $(+1,-K)$ and $(-1,+K)$, in which $\sigma=0$ or ± 1 for torsional levels of symmetry species *A* or *E*, respectively. Transitions shown in Fig. 4 are defined as ${}^{\Delta K}\Delta J_{|K''|}$ for *A* lines and ${}^{\Delta K}J_{K''}$ for *E* lines in which $\Delta K=|K'|-|K''|$. The upper right corner is for labeling the doublet state of K'. Detailed definition of those symbols appears in Refs. 1 and 8. Complete spectra, observed line positions and assignments of all reported bands are given in Ref. 23.

A. $10_0^1 14_0^{0+}$

Lines assigned by Liu *et al.*[15] to be $10_0^1 14_0^{0+}$ were reassigned to be part of band $14_0^{0-} 15_0^2$, according to results of previous work;[1] lines lying to the blue region of those with small spectral intensity are assigned to $10_0^1 14_0^{0+}$ here. The $A-A$ lines of *c* type to the upper states $K=1^{u,l}$ and $2^{u,l}$ are assigned. In this band, the few remaining very weak lines would not be convincingly assigned to sublevel *E*. We expect that, for the lowest torsional level with a moderate barrier, $\Delta_{E-A}\equiv E(E)-E(A)$, is small; hence those $E-E$ lines might severely overlap with $A-A$ lines and be unresolvable under current experimental conditions. For *E* sublevel of 14^{0+} some *b*-type lines with small intensity appear and are separate from the *A* lines. For this band the intensity of these *E* lines might be too small to be confirmed.

The rotational parameter *A* obtained from fitting to an asymmetric rotor is 1.789(1) cm^{-1}, greater than the value obtained for the vibrational ground state 14^{0+}; a large *A* value is expected for a vibrational state with bending excitation. About 21 lines are assigned for this band in the present work. These analyses yield the vibrational frequency $\nu'_{10}=373.163(3)$ cm^{-1} for the C–C–O bending mode, slightly greater than the value obtained by Liu *et al.*[15]

B. $10_0^1 14_0^{0-}$

This band lies in the range of 30 170–30 180 cm^{-1}. Only *a*/*b* hybrid transitions are observed for the $A-A$ lines. Transitions to up to $K=1$ are identified for both torsional sublevels *A* and *E*; in total 68 transitions are assigned for this band. Accordingly, Δ_{E-A} is evaluated to be -0.056 cm^{-1}, with a sign similar to that obtained in the state 14^{0-} but reverse of that in 14^{0+}; its absolute value is slightly greater than that in the other two states. The fitted A_{eff} is 1.595(2) cm^{-1}, similar to the value obtained for 14^{0-}, but small for an excited state involving bending. The effect of torsion on *A*

TABLE I. Band origin, term value, and A/E splitting (cm^{-1}) of $\tilde{A}^1A''$ of CH_3CHO for the 10_0^1 progression.[a]

Band	$\Gamma'-\Gamma''$[b]	K state assigned	Band origin[c]	Term	Δ_{E-A}
$10_0^1 14_0^{0+} 15_0^0$	A_1-A_1	1–2	30 142.208	373.163	
	$E-E$	None			n.a.
$10_0^1 14_0^{0+} 15_0^1$	A_2-A_1	1^l	30 331.591[d]	562.546	
	$E-E$				
$10_0^1 14_0^{0+} 15_0^2$	A_1-A_1	0–2	30 477.900	708.855	
	$E-E$	+1	30 479.605	710.629	1.774
$10_0^1 14_0^{0+} 15_0^3$	A_2-A_1	None			
	$E-E$	0–3	30 613.979	845.003	n.a.
$10_0^1 14_0^{0+} 15_0^4$	A_1-A_1	0	30 709.916	940.871	
	$E-E$	0–1	30 761.989	993.013	52.142
$10_0^1 14_0^{0-} 15_0^0$	A_2-A_1	0–1	30 175.415	406.370	
	$E-E$	0–1	30 175.290	406.314	−0.056
$10_0^1 14_0^{0-} 15_0^1$	A_1-A_1	None			
	$E-E$	0, 1, or −1	30 349.085	580.109	n.a.
$10_0^1 14_0^{0-} 15_0^2$	A_2-A_1	0–1	30 510.992	741.947	
	$E-E$	0	30 509.813	740.837	−1.110
$10_0^1 14_0^{0-} 15_0^3$	A_1-A_1	1–2	30 645.648	876.603	
	$E-E$	None	n.a.	n.a.	n.a.
$10_0^1 14_0^{0-} 15_0^4$	A_2-A_1	0–3	30 742.878	973.833	
	$E-E$	0–1	30 788.278	1019.302	45.469

[a]Uncertainty of the absolute value is 0.004 cm^{-1}; precision of experimental measurement is 0.003 cm^{-1}.
[b]Γ'' and Γ' denote vibrational symmetries for lower and upper states, respectively.
[c]Band origins are determined from experimental transitions, or using the program involving a torsion-rotation ($10^1 14^{0+} 15^2 E$) or an asymmetric Hamiltonian ($10^1 14^{0+} 15^0 A$, $10^1 14^{0-} 15^3 A$).
[d]Band origin is estimated by subtracting 2.090 7 cm^{-1} (separation of 1_{11} and 0_{00} in $10^1 14^{0+}$ state) from transition $J'_{KaKc}-J''_{KaKc}=1_{11}-0_{00}$ (30 333.682 cm^{-1}).

is expected to be negligible for $v_t=0$; a small value of A_{eff} might be due to the rotational structure affected by the inversion motion. Most assignments made by Liu *et al.*[16] are confirmed; because we have an improved signal-to-noise ratio in the present work, more transitions are assigned.

C. $10_0^1 14_0^{0+} 15_0^1$

This band lies in the frequency range 30 325–30 338 cm^{-1}. Only nine $A-A$ transitions are assigned, involving two branches ${}^RR_0^l$ and ${}^QP_{1l}^l$; this analysis yields only the upper state $K=1$, hence a false origin for state 1_{11} lying at 30 333.682 cm^{-1}. No A_{eff} value is determined from assigned transitions, but if we assume that this level has an A_{eff} value similar to that in state $10^1 14^{0+}$, then we obtain an origin $\approx$30 331.591 cm^{-1}. We observe between the two assigned branches a Q branch, which possibly belongs to the E sublevel. No other transitions with reasonable intensity and correct combination differences are found related to this branch to confirm this assignment. Because the intensity of this band is quite distinct from that in band $14_0^{0+} 15_0^1$, no definite rotational assignment is made for the E sublevel. Nearly half the lines assigned by Liu *et al.*[16] for this band are reassigned here; a few weak lines remain unconfirmed.

TABLE II. Effective rotational parameters (cm^{-1}) from an asymmetric rotor fit of the A sublevels of $\tilde{A}^1A''$ of CH_3CHO.

Level	Γ'[a]	$K's$[b]	A_{eff}	B_{eff}	C_{eff}	$D_{JK}\times10^{-4}$	$D_K\times10^{-3}$[c]	$\Delta_N\times10^{-5}$
$10^1 14^{0+}$	A_1	$1^u,1^l,2^u,2^l$	1.789(1)	0.335 8(2)	0.302 7(2)	4.4(7)		
$10^1 14^{0+} 15^1$	A_2	n.a.	n.a.	n.a.	n.a.			
$10^1 14^{0+} 15^2$	A_1	$0,1^u,1^l,2^u,2^l$	1.872(1)	0.339 6(1)	0.296 79(8)	8.5(4)	13.4(3)	
$10^1 14^{0+} 15^3$	A_2	n.a.	n.a.	n.a.	n.a.			
$10^1 14^{0+} 15^4$	A_1	n.a.	n.a.	n.a.	n.a.			
$10^1 14^{0-}$	A_2	$0,1^u,1^l$	1.595(2)	0.339 3(2)	0.296 8(2)	−4(2)		
$10^1 14^{0-} 15^1$	A_1	n.a.	n.a.	n.a.	n.a.			
$10^1 14^{0-} 15^2$	A_2	$0,1^u,1^l$	1.436(1)	0.333 23(7)	0.297 42(6)	13.6(6)		
$10^1 14^{0-} 15^3$	A_1	$1^u,1^l,2^u,2^l$	1.3919(4)	0.325 9(4)	0.314 5(3)			−1.5(7)
$10^1 14^{0-} 15^4$	A_2	$0,1^u,1^l$	7.894(1)	0.338 91(6)	0.306 05(6)	7.2(5)		

[a]Γ' denotes vibrational symmetry.
[b]States included in the fits.
[c]D_K contains a large contribution from the torsional motion.

D. $10_0^1 14_0^{0-} 15_0^1$

This band is nearly 18 cm^{-1} in energy above the position of band $10_0^1 14_0^{0+} 15_0^1$. Our assignments agree with those made by Liu *et al.*[15] The small intensity of this band hampers identifying enough $A-A$ lines to form a complete band, and thus the A/E splitting; in total 27 E transitions are assigned.

E. $10_0^1 14_0^{0+} 15_0^2$

The $A-A$ lines range from 30 472–30 486 cm^{-1}. The rotational structure of this band resembles that in band $14_0^{0+} 15_0^2$, allowing assignments of this band with little trouble. According to assigned transitions of c type up to $K=0$, $1^{u,l}$, and $2^{u,l}$ of sublevel A, A_{eff} of this level is 1.872(1) cm^{-1}, slightly greater than that for $10^1 14^{0+}$; this slight difference in A_{eff} indicates the value of Δ_{E-A} to be smaller than that in $14^{0+}15^2$. According to vibrational assignments, the spacing between $10^1 14^{0+}$ and $10^1 14^{0+} 15^2$ is calculated to be $\approx$337 cm^{-1}, in agreement with $\sim$347 cm^{-1} between 14^{0+} and $14^{0+}15^2$.[1]

According to both spectral intensity and the A/E splitting estimated from the A sublevel, the observed $K=+1$ for E sublevels is assigned to be the upper K doublet state. Four $E-E$ branches ${}^QP_{+1}^+$, ${}^QR_{+1}^+$, ${}^QP_{-1}^+$, and ${}^QR_{-1}^+$ appear with the former two branches having greater spectral intensity than the latter two. These results are consistent with previous findings that $\Delta K=2$ transitions are less probable. In total 43 A and 30 E transitions are assigned for this band.

F. $10_0^1 14_0^{0-} 15_0^2$

This band with origin at 30 510.992(3) cm^{-1} ranges from 30 502–30 516 cm^{-1}. The rotational structure for the A sublevel is similar to that of level $14^{0-}15^2$. Transitions of a/b hybrid type to $K=0$ and $1^{u,l}$ are assigned for sublevel A. Accordingly, A_{eff} is 1.436(1) cm^{-1}, smaller than that for state $10^1 14^{0-}$, and indicating a negative abnormal value of Δ_{E-A} for this state.

In this region, two subbands, $K=0$ and 1 are assigned to E sublevels and are candidates for assignment to this band. For $K=0$ subband, up to six branches are identified in a range 30 505–30 513 cm^{-1}. The $K=1$ subband lies to the red of the $K=0$ subband indicating that they belong to separate vibronic series if one of them is assigned to a $v_t=2$ state. Three branches are assigned for the latter subband. Assigning the $K=0$ subband to $10_0^1 14_0^{0-} 15_0^2$ yields $\Delta_{E-A}=-1.110$ cm^{-1}, whereas assigning $K=1$ to this band yields $\Delta_{E-A}=-3.4$ cm^{-1}. From the obtained A_{eff} and comparison with similar torsional states in other series, the former assignment seems to conform better to experimental data. Overall, 81 A and 20 E transitions are assigned for this band.

G. $10_0^1 14_0^{0+} 15_0^3$

The $E-E$ lines range from 30 606–30 634 cm^{-1}. The spectrum for this band is shown in Fig. 2. Resemblance of rotational structure here to that of $14_0^{0+}15_0^3$ makes lines readily assignable. Transitions up to $K=3$ are assigned; the origin is 30 613.979(3) cm^{-1}. These assignments yield a K

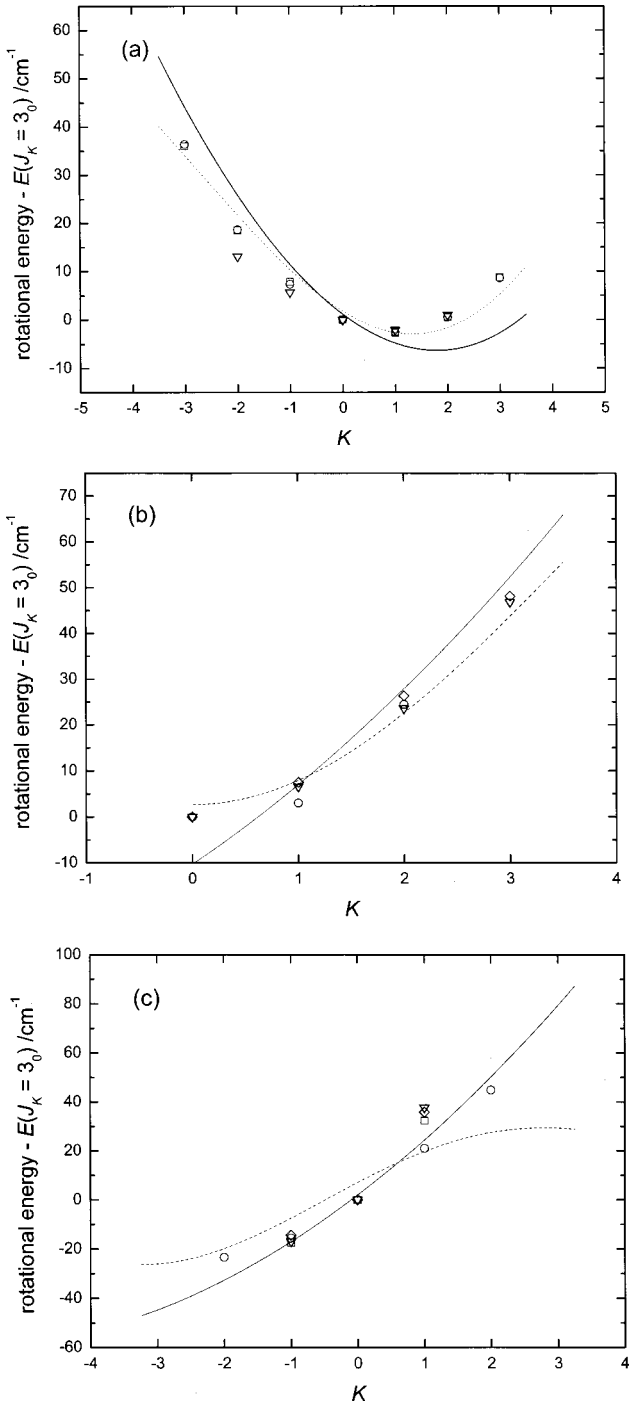

FIG. 5. Plot of rotational energy $-E(J_K)$ vs K for (a) E sublevels of $14^{0+}15^3$ (○), $14^{0-}15^3$ (▽), and $10^1 14^{0+} 15^3$ (□): the solid line is according to Eq. (2) with parameters $F=7.245$, $A-B=1.227$, $V_3=650$, and an offset $=-585.06$, and the dashed line is from the fitted function $16.934\times\cos(2.094\times(K\rho+1))+1.227\times K^2+10.25$. Parameter ρ is fixed at 0.2198. (b) A sublevels of $14^{0+}15^4$ (○), $14^{0-}15^4$ (▽), and $10^1 14^{0-} 15^4$ (◇): the solid line is according to Eq. (2) with a fitted offset $=-640.91$, and the dashed line is from the function $-31.97\times\cos(2.094\times K\rho)+1.1201\times K^2+34.6$. (c) E sublevels of $14^{0+}15^4$ (○), $14^{0-}15^4$ (▽), $10^1 14^{0+} 15^4$ (□), and $10^1 14^{0-} 15^4$ (◇). The solid line is from Eq. (2) with a fitted offset -702.87, and dashed line is from the function $-31.97\times\cos(2.094\times(K\rho+1))+1.1201\times K^2-8.93$. Parameters $F=6.919$, $A-B=1.1201$, $V_3=650$, and $\rho=0.245$ for all lines in (b) and (c). The parameters are in cm^{-1} except ρ has no unit.

$=1$ doublet splitting 10.357 cm^{-1}, comparable to 9.713 cm^{-1} in $14^{0+}15^3$. The K structure here and for states $14^{0+}15^3$ and $14^{0-}15^3$ is shown in Fig. 5(a), displaying similarity to that in $14^{0+}15^3$, but deviating slightly from that in state $14^{0-}15^3$ for rotational levels with negative K values. Total 70 E lines are assigned.

H. $10_0^1 14_0^{0-} 15_0^3$

The A–A lines range from 30 641–30 652 cm^{-1}. Transition of c type with upper state $K=1-2$ are assigned. As shown in Fig. 2, spectral features of A–A transitions resemble those of $14_0^{0-}15_0^3$, but intense E lines are missing from this band; such lines are expected to consist of direct transitions of Franck–Condon c-type and indirect transitions of vibrationally induced a/b type.[24] For this high v_t state, the spectral intensity might be affected by torsional motion: the intensity of E lines is likely accidentally diminished through interaction of torsion, inversion and C–C–O deformation.

According to assignments for A transitions, we obtain $A_{\text{eff}}=1.3919(4)$ cm^{-1}, indicating a negative normal Δ_{E-A} similar to that in $14^{0-}15^3$. The rotational structure for the A sublevel varies slightly; branch ${}^RQ_0^2$ is narrower than in $14_0^{0-}15_0^3$. Similar to $14_0^{0-}15_0^3$, atypical branches ${}^QQ_{1u}^u(J_{1J-1}-J_{1J-1})$, ${}^QQ_{1l}^l(J_{1J}-J_{1J})$, ${}^QR_{1l}^u((J+1)_{1J}-J_{1J})$, ${}^QR_{1u}^l((J+1)_{1J+1}-J_{1J-1})$, ${}^QP_{1l}^u(J_{1J-1}-(J+1)_{1J+1})$, and ${}^QP_{1u}^l(J_{1J}-(J+1)_{1J})$ are observed in the range 30 645.1–30 645.4, 30 646–30 649, and 30 641.5–30 644 cm^{-1}. In total 47 transitions are assigned for this band.

I. $10_0^1 14_0^{0+} 15_0^4$ and $10_0^1 14_0^{0-} 15_0^4$

The most intense features beyond band $14_0^{0-}15_0^4$ are assigned to $10_0^1 14_0^{0+} 15_0^4$ and $10_0^1 14_0^{0-} 15_0^4$; shown in Fig. 1(b), they fall in the range 30 700–30 830 cm^{-1}. For A sublevels, there is only one subband $K=0$, assigned to band $10_0^1 14_0^{0+} 15_0^4$, but for $10_0^1 14_0^{0-} 15_0^4$ the A lines are readily assigned up to $K=3$ in the range 30 736–30 790 cm^{-1}, and with origin at 30 742.878(3) cm^{-1}. The rotational structure of this band is similar to that of band $14_0^{0-}15_0^4$ as shown in Fig. 5(b). The value of A_{eff} fitted for an asymmetric rotor is 7.894(1) cm^{-1} implying a large positive normal Δ_{E-A}.

Because the A/E splittings and K spacings are large for the E sublevels, each band spans a large range and tends to overlap other bands. We distinguish upper and lower $K=1$ and 2 doublets mainly according to spectral intensity in addition to the method of combination differences. Similar to a method used previously,[1] the term value of each K state lying in this range is plotted versus $J(J+1)$. In the region of low vibrational energy, few bands involving other vibrational states exist; from their relative intensity and energy we hence assign most K states to $14^{0+}15^4$ and $14^{0-}15^4$. Like previous assignments,[1] comparison of rotational structures and relatively intensity with those of $14^{0+}15^4$ and $14^{0-}15^4$ enabled us to make the assignments here. About nine K states in the range 30 736–30 835 cm^{-1} are observed; a running number, labeling states in order of energy, is shown in Fig. 6. The E lines with strong intensity are clearly assigned to $10_0^1 14_0^{0-} 15_0^4$ from structure and K spacings similar to those in

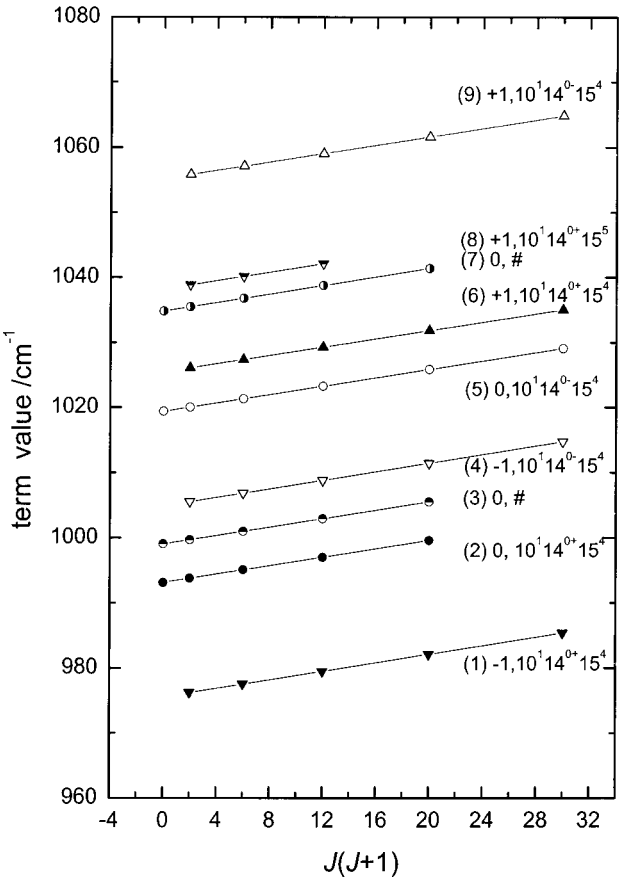

FIG. 6. Plot of observed K stack vs $J(J+1)$ for E sublevels in the region of states $10^1 14^{0+} 15^4$ and $10^1 14^{0-} 15^4$, showing the K structure in the region 970–1060 cm^{-1} above the $\tilde{A}^1A''$ origin. Each state is labeled with a running number (in parentheses), and with K and the vibrational state. Symbol # denotes the unassigned vibrational levels.

$14_0^{0-}15_0^4$. Assignment of K states for $10_0^1 14_0^{0+} 15_0^4$ is more troublesome because large deviations from those in $14_0^{0+}15_0^4$ are found.

State 4 ($K=-1$) comprising ten branches in the range 30 765–30 778 cm^{-1} and state 9 ($K=+1$) at 30 820–30 828 cm^{-1} having rotational structures similar to that in $14^{0-}15^4$ are assigned to $10^1 14^{0-} 15^4$. Accordingly, the $K=1$ doublet splitting is 50.31 cm^{-1}, comparable to 54.61 cm^{-1} in $14_0^{0-}15_0^4$. State 5 ($K=0$) with origin 30 788.278(3) cm^{-1} is about 45.469 cm^{-1} from the A sublevel of $10_0^1 14_0^{0-} 15_0^4$, in agreement with $\Delta_{E-A}=48.798$ cm^{-1} for $14_0^{0-}15_0^4$. Hence, this state is assigned to $10^1 14^{0-} 15^4$.

State 1 extending over 30 740–30 750 cm^{-1} is assigned to $K=-1$ of $10_0^1 14_0^{0+} 15_0^4$ from its rotational structure and energy relative to nearby states. States 2, 3, and 7 are all assigned to $K=0$ with origins at 30 761.989(3), 30 767.947(3), and 30 803.735(3) cm^{-1}, respectively. Transitions to state 2, assigned to $10_0^1 14_0^{0+} 15_0^4$, yield an A/E splitting 52.142 cm^{-1}, greater than 45.437 cm^{-1} for $14^{0+}15^4$, but closer to 48.798 cm^{-1} for $14^{0-}15^4$. Assigning either state 3 or 7 to $10^1 14^{0+} 15^4$ would yield a value of Δ_{E-A}, too large to be justified. Hence we assign state 2 to $10^1 14^{0+} 15^4$; vibrational assignments of states 3 and 7 are unknown. State 8 is assigned to $K=+1$ of $10^1 14^{0+} 15^5$.

We assigned state 6 to $K=+1$ of $10_0^1 14_0^{0+} 15_0^4$; accordingly, the $K=1$ splitting is 49.863 cm^{-1}, greater than 36.621 cm^{-1} found in $14^{0+}15^4$, but near 54.61 cm^{-1} in $14^{0-}15^4$. For torsional states lying at the barrier, slight variation of the height of the barrier affects significantly the K doublet spacing. The K structure of $10^1 14^{0+} 15^4$, along with other states for comparison, is plotted versus K as shown in Fig. 5(c). States $14^{0-}15^4$, $10^1 14^{0+} 15^4$, and $10^1 14^{0-} 15^4$ show similar structure, with small deviations, but all deviate significantly from that in $14^{0+}15^4$. In total 13 and 149 A lines and 53 and 88 E lines are assigned for $10_0^1 14_0^{0+} 15_0^4$ and $10_0^1 14_0^{0-} 15_0^4$, respectively.

III. DISCUSSION

A. Rotational structure

For a nearly prolate rotor, the rotational energy of a torsional level deep in the well is expressed approximately[8] as

$$E_{\text{tor},K\text{-rot}} = Fa_1 \cos[(2\pi/3)(K\rho+\sigma)] + (A-\overline{B})K^2, \quad (1)$$

$\rho \sim 0.3$ for acetaldehyde; for A sublevels $\sigma=0$, and for E $\sigma=+1$ and -1. The effective rotational parameter for internal rotation is F. In the free-rotor limit, the torsion-rotational energy is expressed approximately[10] as

$$E_{f,K\text{-rot}} = F(m+\rho K)^2 + (A-\overline{B})K^2 + E^{(2)}, \quad (2)$$

$$E^{(2)}(m,K) = V_3/2 + 18(V_3/4)^2/F[36(m+\rho K)^2 - 81], \quad (3)$$

in which m is the free-rotor quantum number; both m and K are signed integers. The sign of K is defined relative to the sign of m in free rotor [Eq. (2)] different from the convention for torsional level.[10] Comparing both conventions, we used $F(m-\rho K)^2$ (here m is kept positive) to replace the first term in Eq. (2) for the odd v_t states. The second-order perturbation correction to free-rotor energies is, $E^{(2)}(m,K)$ arising from a term for the nonzero barrier $(1/2)V_3(1-\cos 3\gamma)$.[10] For states $v_t=0-2$ lying below the barrier, the experimental data follow approximate results based on Eq. (1). Because states $v_t=3$ and 4 lie near the top of the barrier, they are considered to fall in the intermediate region between limits of a high-barrier torsion and a free rotor. We compare the measured K structure of states to these limiting cases based on Eqs. (1) and (2). In the fits, only an offset to total energy was varied; ρ, Fa_1 and rotational constants for various torsional states obtained from previous work[1] were kept fixed during the fits. The offset from Eq. (1) to the experimental data contains high-order terms and the deviation from rotational energy at $J_K=3_0$. From Eq. (2) the offset includes correction to total vibrational energy and zero-point energy.

The results of fits and experimental data are shown in Fig. 5. Clearly, the experimental data deviate from both, limiting case behaviors. However, for sublevels $v_t=3E$ and $v_t=4A$, the experimental data are near the high-barrier limit, but for $v_t=4E$ near a free rotor. These comparisons show that although $v_t=4A$ lies near the top of the torsional barrier, its K structure behaves close to that predicted from the high-barrier limit. State $v_t=4E$ lying only 45–50 cm^{-1} above the state $v_t=4A$, but exceeding the torsional barrier behaves closer to a free rotor. Nevertheless for both, $v_t=3E$ and $v_t=4A$, including some character of free rotor, whereas for $v_t=4E$ including some character of the high barrier vibrational state, would yield better empirical fits to the experimental data.

Comparing the detailed K structure, for E sublevels, we find that $10^1 14^{0+} 15^3$ agrees with $14^{0+}15^3$ but deviates from $14^{0-}15^3$. Structures for levels $14^{0+}15^4$, $14^{0-}15^4$, $10^1 14^{0+} 15^4$, and $10^1 14^{0-} 15^4$ are displayed in Fig. 5(c); clearly $14^{0+}15^4$ deviates from the other three. The K structure is sensitive to the height of the torsion barrier; the geometry of various vibrational combination states can differ slightly, causing the barrier height to vary. These experimental data display clearly that interaction of inversion; C–C–O bend and torsion perturbs the structure of rotation. Although there exists small deviations among the combination vibrational states, states of the same v_t display the same qualitative behavior with respect to their approaching either the high-torsional barrier or free-rotor limit.

B. Torsion-inversion-bending energy levels

From the origin of band $10_0^1 14_0^{0+} 15_0^0$ the vibrational frequency of C–C–O bend is obtained to be 373.163 cm^{-1}. Because the transition to state $\tilde{A}^1A''$ is an n-π^*, this vibrational frequency is, as expected, significantly smaller than that for the electronic ground state ($\nu''_{10}=509$ cm^{-1}).[25]

The values of the effective rotational parameters for the $10^1 14^{0+}$ and $10^1 14^{0-}$ series are listed in Table II; the fitted B and C parameters are similar to those in series 14^{0+} and 14^{0-} but the values of the parameter A_{eff} obtained for the series $10^1 14^{0+}$ are greater than those of series 14^{0+}. A large value for the rotational parameter A is expected for vibrationally excited state involving the bending motion, but for $v_t=0$ and 2 in series $10^1 14^{0-}$, the fitted A_{eff} is similar to those in series 14^{0-}. For these states with small torsional quantum number, the effect on the rotational parameter A by the torsional motion is minimal, so that some interaction of the inversion with Q_{10} in these combination states may arise, which affects the K rotational structure, and consequently alters the fitted effective rotational parameters.

Torsional spacings among these torsional states obtained for series $10^1 14^{0+}$ and $10^1 14^{0-}$ are generally slightly smaller than those for states in series 14^{0+} and 14^{0-}, as shown in Table III. Upon excitation of the C–C–O bend, the molecule stays at large angles with increased probability; hence, on average, decreased constraint of torsional motion is expected, accordingly a small torsion frequency and barrier height.

Because inversion and torsion interact, the inversion spacing between the 14^{0+} and 14^{0-} states decreases abruptly from $\approx$34.37 cm^{-1} for $v_t=0$ to a small value 17.080 (A) and 17.397 cm^{-1} (E) for $v_t=1$ in the same series, then reverts to 30–33 cm^{-1} for $v_t=4$. Similarly, the spacing between the $10^1 14^{0+}$ and $10^1 14^{0-}$ series is 33.207 cm^{-1} for $v_t=0A$ and 17.56 cm^{-1} for $v_t=1$ (estimated roughly from the difference between $10^1 14^{0+} 15^1 A$ and $10^1 14^{0-} 15^1 E$; here we assume that the Δ_{E-A} is small both states). Resulting from interaction with inversion, 14^{0+} components of both 15^1 and $10^1 15^1$ are elevated from their original positions and

TABLE III. Term values and torsional and inversion energy separation (cm^{-1}) of $\tilde{A}^1A''$ of CH_3CHO for series 14^{0+}, 14^{0+}, 10^114^{0+}, and 10^114^{0-}.

		14^{0+}[a]		14^{0-}[a]		$14^{0+}/14^{0-}$	10^114^{0+}		10^114^{0-}		$10^114^{0+}/10^114^{0-}$
v_t	Sublevel	Term[b]	Δ_t[c]	Term[b]	Δ_t[c]	Δ_{inv}[c]	Term[b]	Δ_t[c]	Term[b]	Δ_t[c]	Δ_{inv}[c]
0	*A*	0		0		34.370	0		0		33.207
	E	0.004		−0.003		34.363	n.a.		−0.056		n.a.
1	*A*	193.474	193.474	176.184	176.184	17.080	189.383	189.383	n.a.	n.a.	
	E	193.190	193.186	176.217	176.220	17.397	n.a.	n.a.	173.739	173.795	(17.563)[d]
2	*A*	346.662	153.188	337.846	161.662	25.554	335.692	146.309	335.577	n.a.	33.092
	E	348.822	155.632	337.511	161.294	23.059	337.466	n.a.	334.467	160.728	30.208
3	*A*	n.a.	n.a.	485.327	147.481	n.a.	n.a.	n.a.	470.233	134.656	n.a.
	E	483.106	134.284	476.290	138.779	27.554	471.840	134.374	n.a.	n.a.	n.a.
4	*A*	573.050	n.a.	568.707	83.38	30.027	567.708	n.a.	567.463	97.230	32.962
	E	618.487	135.381	617.505	141.215	33.388	619.850	148.010	612.932	n.a.	26.289

[a]Data obtained from previous work (Ref. 1).
[b]Term value is defined to be energy relative to the origin in its series.
[c]Δ_t=torsional energy spacing and Δ_{inv}=energy between two inversion components 14^{0+} and 14^{0-}.
[d]Obtained from separation between $10^114^{0+}15^1(A)$ and $10^114^{0-}15^1(E)$.

display large torsional spacings, whereas 14^{0-} components ($14^{0-}15^1$ and $10^114^{0-}15^1$) maintain a regular spacing; hence the spacing between these two inversion components 14^{0+} and 14^{0-} is small for $v_t=1$ states. For $v_t=2$ the inversion spacing reverts to a regular value of about 30–33 cm^{-1} for the 10^1 series, whereas for the pure torsional series 14^{0+} and 14^{0-} the inversion does not become regular until $v_t=4$. According to the present experimental data, and as might be expected, the effect of the large amplitude inversion motion on the torsional levels and rotational structure is more significant than that of the smaller amplitude bending motion in the electronic excited state.

C. Other vibrational bands

In the present work we assigned most levels with vibrational energy up to 1000 cm^{-1}, but levels involving other vibrational motion are also accessible. Bands $10_0^214_0^{0+}$ and $10_0^214_0^{0-}$ are expected to appear in the region with energy similar to that of $10_0^114_0^{0-}15_0^2$, but no $A-A$ lines are assigned to these two bands in that vicinity. Several $E-E$ lines appear, but we make no definite vibrational assignments for those lines here. Relative to the spectra in bands $10_0^114_0^{0+}$ and 14_0^{0+}, the A lines display greater intensity than E lines, so we would expect bands $10_0^214_0^{0+}$ and $10_0^214_0^{0-}$ to have intense A lines. Hence series 10^2 are not assigned here.

A vibrational progression involving 14^{1+} is expected to appear first about 400–500 cm^{-1} above the origin of $\tilde{A}^1A''$. These two bands at 30 258 cm^{-1} and at 30 276–30 280 cm^{-1} are assigned by Nobel and Lee[22] and by Liu *et al.*,[16] respectively, to be $14_0^{1+}15_0^0$, but in our previous work[1] we reassigned them to $14_0^{0+}15_0^3$ and $14_0^{0-}15_0^3$, respectively. Baba *et al.*[2] assigned a band at 30 176 cm^{-1} to the state with inversion excitation, but we reassign this band here to $10_0^114_0^{0-}$. An unassigned progression lying to the blue of 10^114^{0-} likely involves 14^{1+} because it lies in the expected energy region and because there is no 14^{0-} component lying $\approx$30 cm^{-1} apart. Because the barrier for inversion is relatively small, the other component 14^{1-} is expected to lie far away from 14^{1+}. States with $v_t=5-6$ that exist in the high-energy region also require assignment. Those states tend to extend over a wide energy and interfere with assignments of other progressions. Further analyses on the spectrum for those free-rotor states are required prior to elucidating the other combination states.

IV. CONCLUSION

Assignments in the previous work of combination vibrational states involving C–C–O deformation agree roughly with those made by Nobel and Lee.[22] From a full analysis of rotational and vibrational structures, the torsional and inversion spacings and rotational structures are found to be similar to those in the 14^{0+} and 14^{0-} series, but some deviations are observed from the pure torsional series; e.g., E lines are intense in $14^{0-}15^3$ but disappear entirely in $10^114^{0-}15^3$. Comparison of the four series studied, i.e., 14^{0+}, 14^{0-}, 10^114^{0+}, and 10^114^{0-}, indicates that the K structure of $14^{0+}15^3$ resembles that of $10^114^{0+}15^3$, more than that of $14^{0-}15^3$; states $14^{0-}15^4$, $10^114^{0+}15^4$, and $10^114^{0-}15^4$ have similar rotational structure but all differ from that of $14^{0+}15^4$. The K rotational structures of $v_t=3$ E and $v_t=4$ A of all series retain resemblance to a high-barrier torsional vibrational state. For $v_t=4$ E, the states which surpass the torsional barrier behave like free-rotor states.

From our treatment of the experimental data, we conclude that interaction of the C–C–O bend with torsional states is smaller than that of the aldehyde inversion in terms of rotational structure and torsional spacing, but the effect on spectral intensity for some bands is still significant. Our new experimental data provide detailed results on the vibrational and rotational structures of torsional levels involving the inversion and bending vibrational motions. A theory concerning interaction of torsional and other vibrational motion is required to resolve the many subtle problems impeding full understanding of the spectral data. The abnormal Δ_{E-A} splitting for $v_t=0-2$ is attributed to interaction of torsion and inversion. The study on quantitative analysis of these splittings and explanation is in progress.

ACKNOWLEDGMENTS

The authors (Y.-C.C., C.-L.H., and I.-C.C.) thank Isabelle Kleiner for providing the program, Jon Hougen for helpful discussion, and the National Science Council and Ministry of Education of Republic of China for financial support. The authors (C.-K.N. and A.H.K.) thank NSC and China Petroleum Company, Taiwan for partial support.

[1] Y.-C. Chou, C.-L. Huang, I.-C. Chen, C.-K. Ni, and A. H. Kung, J. Chem. Phys. **115**, 5089 (2001).
[2] M. Baba, I. Hanazaki, and U. Nagashima, J. Chem. Phys. **82**, 3938 (1985).
[3] J. C. D. Brand, J. Electrochem. Soc. **1956**, 858.
[4] H. Hollenstein and F. Winther, J. Mol. Spectrosc. **71**, 118 (1978).
[5] W. Liang, J. G. Baker, E. Herbst, R. A. Booker, and F. C. Delucia, J. Mol. Spectrosc. **120**, 298 (1986).
[6] I. Kleiner, M. Godefroid, M. Herman, and A. R. W. McKellar, J. Mol. Spectrosc. **142**, 238 (1990).
[7] I. Kleiner, J. T. Hougen, R. D. Suenram, F. J. Lovas, and M. Godefroid, J. Mol. Spectrosc. **148**, 38 (1991).
[8] J. T. Hougen, I. Kleiner, and M. Godefroid, J. Mol. Spectrosc. **163**, 559 (1994).
[9] S. P. Belov, M. Y. Tretyakov, I. Kleiner, and J. T. Hougen, J. Mol. Spectrosc. **160**, 61 (1993).
[10] I. Kleiner, J. T. Hougen, J.-U. Grabow, S. P. Belov, M. Y. Tretyakov, and J. Cosleou, J. Mol. Spectrosc. **179**, 41 (1996).
[11] J. Ortigoso and J. T. Hougen, J. Chem. Phys. **101**, 2710 (1994).
[12] J. Ortigoso, I. Kleiner, and J. T. Hougen, J. Chem. Phys. **110**, 11688 (1999).
[13] M. A. Mekhtiev and J. T. Hougen, J. Mol. Spectrosc. **187**, 49 (1998).
[14] J. Ortigoso and J. T. Hougen, J. Chem. Phys. **112**, 10212 (2000).
[15] H. Liu, E. C. Lim, C. Muñoz-Caro, A. Niño, R. H. Judge, and D. C. Moule, J. Mol. Spectrosc. **175**, 172 (1996).
[16] H. Liu, E. C. Lim, A. Niño, C. Muñoz-Caro, R. H. Judge, and D. C. Moule, J. Mol. Spectrosc. **190**, 78 (1998).
[17] E. Jalviste, G. Berden, M. Drabbels, and A. M. Wodtke, J. Chem. Phys. **114**, 8316 (2001).
[18] X. Wang and D. S. Perry, J. Chem. Phys. **109**, 10795 (1998).
[19] X. Q. Tan, W. A. Majewski, D. F. Plusquellic, and D. W. Pratt, J. Chem. Phys. **94**, 7721 (1992).
[20] X. Q. Tan and D. W. Pratt, J. Chem. Phys. **100**, 7061 (1994).
[21] H. Zuckermann, Y. Haas, M. Drabbels, J. Heinze, W. Leo Meerts, J. Reuss, and J. van Bladel, Chem. Phys. **163**, 193 (1992).
[22] M. Noble and E. K. C. Lee, J. Chem. Phys. **81**, 1632 (1984).
[23] See EPAPS Document No. E-JCPSA6-116-010202 for figures and tables containing spectra and lists of positions of reported bands. This document may be retrieved via the EPAPS homepage (http://www.aip.org/pubservs/epaps.html) or from ftp.aip.org in the directory /epaps/. See the EPAPS homepage for more information.
[24] R. A. Weersink, D. T. Cramb, S. C. Wallace, and R. D. Gordon, J. Chem. Phys. **102**, 623 (1995).
[25] H. Hollenstein and Hs. H. Günthard, Spectrochim. Acta, Part A **27**, 2027 (1971).